AIMS Mathematics

https://www.aimspress.com/journal/Math

AIMS Mathematics, 11(9): 30280–30303.
DOI: 10.3934/math.20261200
Received: 24 July 2026
Revised: 30 August 2026
Accepted: 14 September 2026
Published: 17 September 2026

Research article

Observer-based neural integral sliding mode control for singular Markovian jump systems against actuator spoofing attacks

Zhihao Wang, Xuetong Zhang, Zihan Zhao, and Guangming Zhuang*

Department of Mathematics and Systems Science, Liaocheng University, Liaocheng 252059, China

* **Correspondence:** Email: zgmtsg@126.com.

Abstract: This paper develops an observer-based neural integral sliding mode control scheme for singular Markovian jump systems subject to malicious actuator spoofing attacks. Vulnerabilities in network transmissions enable adversaries to tamper with the control signals, which substantially degrades the system's operational performance and may even lead to closed-loop instability. A three-layer feedforward neural network is adopted to approximate unknown nonlinear attack signals, where prior knowledge of the attack's upper bounds is not required. To reconstruct immeasurable system states, a mode-dependent sliding mode observer is established. An integral sliding surface with continuous value inheritance at Markovian switching instants is designed to eliminate jumps of the sliding variables induced by mode transitions. A novel neural sliding mode control law is formulated to guarantee the finite-time reachability of the sliding manifold. By virtue of the weak infinitesimal generator and linear matrix inequality techniques, tractable sufficient conditions are derived to ensure the stochastic admissibility of the closed-loop system. Finally, a practical engineering example of a direct current motor is presented to validate the state estimation, anti-attack, and steady-state tracking performance of the developed control strategy.

Keywords: singular Markovian jump systems; actuator spoofing attacks; neural network approximation; integral sliding mode control; sliding mode observer; stochastic admissibility
Mathematics Subject Classification: 93C57, 68T07

1. Introduction

Singular systems are also referred to as generalized descriptor systems, which are governed by coupled algebraic and differential equations. Such characteristics enable accurate modeling for many industrial devices, including direct current (DC) motors, vehicle suspension devices, and power networks [1–3]. Compared with conventional regular state-space systems, singular systems must simultaneously satisfy three critical properties, namely regularity, an impulse-free property, and stochastic stability, which greatly increases the difficulty of stability analysis and controller design [4–6]. When the system's load, internal structure, or component parameters mutate randomly, singular systems can be modeled as singular Markovian jump systems (SMJSs), a typical class of stochastic hybrid systems governed by continuous-time Markov switching processes [7–9].

Networked control systems (NCSs) send measurement data and control commands over public communication channels. This working pattern provides benefits such as a low wiring cost and a flexible layout [10, 11]. Meanwhile, it also brings serious cybersecurity risks [12–14]. Malicious attackers can intercept network data packets and inject false signals into the actuator channels, namely actuator spoofing attacks [15–17]. Such manipulated control inputs will lead to large steady-state tracking errors, serious transient oscillation and even closed-loop instability [18–20]. Therefore, resilient anti-attack control for networked SMJSs has become a vital research direction in reliability engineering and system safety [21, 22].

In most existing relevant research, adaptive parameter identification methods are commonly utilized to counteract time-varying unknown system parameters [23–25]. Nevertheless, such adaptive schemes bring extra dynamic states for online parameter tuning, leading to heavy real-time computation loads [26]. Moreover, improperly set adaptive gains tend to trigger violent control oscillation and slow convergence [27–29]. In practical industrial scenarios, physical calibration tests can determine the fluctuation range of a system's parameters [30–32]. Parameter deviations can then be described by structured bounded uncertainty [33–35]. Fixed constant bounding matrices are defined for each system operation mode. Inspired by practical engineering characteristics and robust control theories, this paper discards all adaptive parameter update rules [36–38]. Instead, linear matrix inequality-based robust bounding techniques are adopted to suppress parameter perturbations, simplifying Lyapunov functional construction and lowering the online computational complexity greatly [39–41].

Sliding mode control (SMC) possesses inherent strong robustness against matched disturbances and parametric variations, and has been extensively applied to Markov jump and singular systems [42]. Traditional fixed sliding surfaces independent of switching modes will bring large conservatism for SMJSs with obvious dynamic differences among modes. Mode-dependent sliding surfaces can match the dynamic characteristics of each operation mode, but mode switching may cause the discontinuity of sliding variables and unexpected state impulses [43, 44]. Integral sliding terms with value inheritance at switching instants can effectively suppress such jump phenomena [45].

Nevertheless, most existing SMC results for SMJSs assume all system states are fully measurable, which cannot be satisfied in actual equipment where the speed and displacement sensors are expensive or unavailable. It is necessary to construct sliding mode observers to reconstruct unmeasurable state information. Most existing observer-based SMC schemes for SMJSs deal mainly with lumped external disturbances. Different from these existing results [46, 47], this paper investigates unknown nonlinear actuator spoofing attacks. A neural network (NN) approximator is adopted to compensate for attack signals. This approach does not require prior information about the attack's upper bounds. Besides, the developed mode-dependent integral sliding surface with value inheritance at switching instants can eliminate undesired sliding variable jumps triggered by Markovian mode transitions, which are rarely taken into account in prior observer-based SMC frameworks.

For unknown nonlinear actuator attacks, a common restrictive precondition requires the upper bound of attack functions to be known in advance, which is unrealistic in real attack scenarios [48, 49]. NNs's own universal approximation ability for continuous nonlinear functions on compact sets, which can approximate unknown attack signals without prior bounded information [50, 51]. Nevertheless, few existing research works integrate mode-dependent sliding mode observers, NN attack compensators and structured norm-bounded uncertainty suppression for SMJSs, which motivates the present paper [52].

The main contributions of this paper are summarized as follows:

(1) A three-layer feedforward NN is adopted to approximate unknown actuator spoofing attacks, removing the restrictive assumption of known attack-related upper bounds. A static NN compensation term is designed without dynamic adaptive laws for NNs' weights, and the sliding mode observer simultaneously compensates for structured parametric uncertainties and NN approximation residual errors to realize high-precision state reconstruction.
(2) A mode-dependent integral sliding surface with continuous inheritance of the integral terms at Markov switching moments is constructed to eliminate sliding variable jumps caused by mode switching. The proposed neural SMC law ensures the finite-time reachability of the sliding manifold in the almost-sure mean-square sense.
(3) Based on the weak infinitesimal generator of Markov jump stochastic processes, improved Lyapunov functionals are constructed, and tractable linear matrix inequation (LMI)-based sufficient conditions are derived to guarantee the stochastic admissibility of the closed-loop SMJS. Two typical mechanical examples are provided to verify the superiority of the proposed scheme in state estimation, structured uncertainty rejection, and actuator attack suppression.

Notation. The symmetric matrix $X > 0$ ($X < 0$) implies that X is a positive-definite (negative-definite) matrix, $\lambda(\cdot)$ denotes the eigenvalues of the corresponding matrix, and $\|\cdot\|$ and $\|\cdot\|_1$ denote the matrix two- and one-norm, respectively. The symbol sym(X) refers to $X + X^{\mathrm{T}}$, Ω denotes the regressor vector for the NNs' approximation residual, S_c represents the auxiliary error-driven signal for adaptive updating laws and λ_{gh} is the Markov mode transition rate.

2. Problem formulation

2.1. System description

Consider the following SMJS with the structured norm-bounded parametric uncertainties:

$$\begin{cases} E\dot{x}(t) = [A(\xi_t) + \Delta A(\xi_t, t)]x(t) + B(\xi_t)\bar{u}_a(t), \\ \ \ y(t) = C(\xi_t)x(t), \end{cases} \tag{2.1}$$

where $x(t) \in \mathbb{R}^n$ denotes the system state vector, $\bar{u}_a(t) \in \mathbb{R}^m$ is the corrupted actuator input suffering network attacks and $y(t) \in \mathbb{R}^p$ represents the measurable output vector. The singular matrix $E \in \mathbb{R}^{n\times n}$ satisfies rank$(E) = \sigma < n$. $\{\xi_t, t \geq 0\}$ stands for a right-continuous Markov switching stochastic process taking values in the finite set $\mathcal{A} = \{1, 2, \ldots, N\}$. For any mode $\xi_t = g \in \mathcal{A}$, the constant matrices A_g, B_g and C_g are known, and B_g is of full column rank.

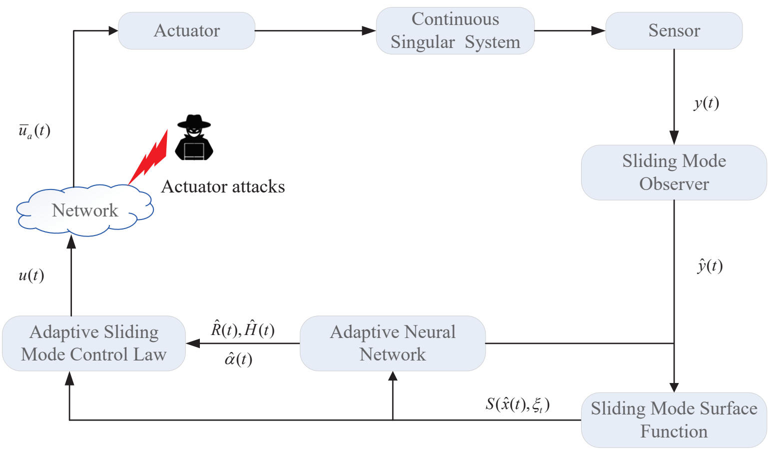

Figure 1. Framework of singular MJSs under spoofing attacks.

The time-varying parametric uncertainty matrix $\Delta A(g, t)$ satisfies the following structured norm-bounded form:

$$\Delta A(g, t) = M_g F(t) N_g, \quad F^{\mathrm{T}}(t) F(t) \leq I, \quad \forall\, t \geq 0, \tag{2.2}$$

where $M_g \in \mathbb{R}^{n \times h}$, $N_g \in \mathbb{R}^{l \times n}$ are known constant bounding matrices for each mode, and $F(t) \in \mathbb{R}^{h \times l}$ is an unknown time-varying matrix function without other prior constraints.

Due to malicious data injection over communication networks, the actual control signal received by the actuator is contaminated, which is formulated as:

$$\bar{u}_a(t) = u(t) + \vartheta(x(t), t), \tag{2.3}$$

where $u(t)$ is the control law to be designed, and $\vartheta(x(t), t)$ denotes the unknown nonlinear actuator spoofing attack function defined on compact set $\Im \subset \mathbb{R}^n$.

2.2. *NN approximation for unknown actuator attacks*

The unknown continuous nonlinear attack term $\vartheta(x(t), t)$ can be approximated by a three-layer feedforward NN on the compact set $\Im$:

$$\vartheta(x(t), t) = R^{*T} \Phi(H^{*T} \bar{O}) + \psi(x), \quad x(t) \in \Im, \tag{2.4}$$

where the NN input vector $\bar{O} = [x(t)^{\mathrm{T}}, -1]^{\mathrm{T}}$, $\tilde{X}_d$ is the number of hidden layer neurons, and $H^* \in \mathbb{R}^{(n+1) \times \tilde{X}_d}$ and $R^* \in \mathbb{R}^{\tilde{X}_d \times m}$ are the optimal input-hidden and hidden-output weight matrices; the sigmoid activation function is selected as

$$\Phi_i(c_i) = \frac{1}{1 - e^{-m_i c_i}}, \quad m_i > 0,$$

and $\psi(x)$ represents the NNs' residual approximation error satisfying $\|\psi(x)\| \leq O$ with an unknown constant $O > 0$. Since the optimal weights H^*, R^* are unavailable in practice, the constant static estimated weight matrices $\hat{H}, \hat{R}$ are adopted to construct the attack compensator:

$$\hat{\vartheta}(x(t), t) = \hat{R}^{\mathrm{T}} \Phi(\hat{H}^{\mathrm{T}} \bar{O}). \tag{2.5}$$

The approximation error is defined as $\tilde{\vartheta} = \hat{\vartheta} - \vartheta$, and the residual norm satisfies $\|\tilde{\vartheta}(x)\| \leq \alpha^{\mathrm{T}}\Omega$, where the constant vector $\alpha \in \mathbb{R}^4$ and the regressor vector $\Omega = (1, \|\bar{O}\|, \|\bar{O}\|\|\hat{R}\|_F, \|\bar{O}\|\|\hat{H}\|_F)^{\mathrm{T}}$. No dynamic adaptive updating laws are designed for the NN weights $\hat{H}, \hat{R}$.

In this work, the sigmoid activation function is adopted mainly for two considerations. First, the sigmoid function is continuously differentiable over the entire real domain, which avoids non-differentiable points brought by Rectified Linear Unit (ReLU) and guarantees the mathematical feasibility of Lyapunov-theoretic derivation for SMJSs. Second, its output is bounded within $(0, 1)$ [16]. Such bounded property helps constrain the output amplitude of the neural approximator, which is favorable for the stability analysis of the considered system. By contrast, ReLU suffers from non-differentiability at zero, and the output range $(-1, 1)$ of tanh does not match our magnitude-constrained approximation requirement. For these reasons, the sigmoid function is selected in our NN.

The number of hidden-layer neurons is chosen by balancing function approximation accuracy and online computational complexity. Too few hidden-layer neurons will degrade the fitting capability and yield large approximation residuals for unknown nonlinear actuator spoofing attacks, whereas excessive neurons impose heavy computational burden and may cause over-fitting. In this work, 20 hidden-layer neurons are determined via trial-and-error tests to achieve satisfactory approximation performance with acceptable computational overhead [22, 24].

2.3. *Definitions*

(1) [1] The unforced singular system $E\dot{x} = (A_g + \Delta A_g)x$ is regular and impulse-free if the matrix pair $(E, A_g + M_g F(t) N_g)$ is regular and impulse-free for all $g \in \mathcal{A}$ and admissible $F(t)$ satisfying $F^{\mathrm{T}}F \leq I$.

(2) [1] The unforced SMJS is mean-square stochastically stable if for any initial state x_0 and initial mode ξ_0,

$$\mathbb{E}\left\{ \int_0^{+\infty} \|x(t)\|^2 dt \,\middle|\, x_0, \xi_0 \right\} < +\infty. \tag{2.6}$$

(3) [1] The SMJS is stochastically admissible if it simultaneously satisfies regularity, impulse-free property and mean-square stochastic stability.

3. Results

3.1. *Mode-dependent sliding mode observer design*

In practical engineering, full state measurement is often unavailable, and thus a mode-dependent sliding mode observer is constructed to reconstruct unmeasurable system states:

$$\begin{cases} E\dot{\hat{x}}(t) = [A_g + M_g F(t) N_g]\hat{x}(t) + B_g(u(t) + u_f(t)) + L_g(y(t) - C_g\hat{x}(t)), \\ \hat{y}(t) = C_g\hat{x}(t), \end{cases} \tag{3.1}$$

where $\hat{x}(t) \in \mathbb{R}^n$ denotes the state estimation vector, $L_g \in \mathbb{R}^{n\times p}$ is the mode-dependent observer gain matrix to be solved via LMIs, and $u_f(t)$ is the robust compensation term for actuator attacks and NN residual errors.

Define the state estimation error as

$$e(t) = x(t) - \hat{x}(t). \tag{3.2}$$

Subtracting the observer dynamics from the original singular Markov jump system, it is seen that

$$\begin{aligned} E\dot{e}(t) &= E\dot{x}(t) - E\dot{\hat{x}}(t) \\ &= \left[A_g x(t) + B_g(u(t) + \vartheta(x,t)) + M_g F(t) N_g x(t)\right] \\ &\quad - \left[A_g \hat{x}(t) + B_g(u(t) + u_f(t)) + L_g(y(t) - C_g \hat{x}(t))\right]. \end{aligned} \tag{3.3}$$

Canceling the common control input term $B_g u(t)$, substituting the output equation $y(t) = C_g x(t)$ into the expression above, we can obtain

$$E\dot{e}(t) = A_g(x(t) - \hat{x}(t)) + M_g F(t) N_g x(t) + B_g \vartheta(x,t) - B_g u_f(t) - L_g(C_g x(t) - C_g \hat{x}(t)). \tag{3.4}$$

Noting that $x(t) = \hat{x}(t) + e(t)$, substituting $x(t) = \hat{x}(t) + e(t)$ into the uncertainty term, it yields that

$$M_g F(t) N_g x(t) = M_g F(t) N_g(\hat{x}(t) + e(t)).$$

Consequently, we obtain

$$E\dot{e}(t) = (A_g + M_g F(t) N_g - L_g C_g) e(t) + B_g(\vartheta(x,t) - u_f(t)). \tag{3.5}$$

All structured parametric uncertainty terms $M_g F(t) N_g$ are lumped into the state and error dynamics, and Lemma 2.1 is utilized to eliminate the unknown time-varying matrix $F(t)$ without any online parameter adaptive laws.

3.2. Mode-dependent integral sliding surface

Construct an integral sliding surface varying with the Markov switching mode g:

$$s(\hat{x}(t), g) = B_g^{\mathrm{T}} G_g E \hat{x}(t) - \int_0^t B_g^{\mathrm{T}} G_g [A_g + M_g F(\tau) N_g + B_g K_g] \hat{x}(\tau) d\tau, \tag{3.6}$$

where $G_g > 0$ and K_g are the positive definite matrix and state-feedback gain matrix to be designed. At the Markov switching instant t_s where the mode switches from g to h, the integral term inherits the terminal value of the previous mode, i.e., $I_h(t_s) = I_g(t_s)$.

This inheritance mechanism ensures that the sliding variable $s(\hat{x}(t), g)$ is continuous at the switching moments and eliminates impulsive state jumps induced by mode switching.

Remark 1. *For numerical implementation in a simulation, once a Markovian mode-switching instant t_s is detected, the integral accumulator variable retains its terminal value computed from the previous mode at t_s^-, and this terminal value is assigned as the initial condition of the integral term for the new mode starting from t_s^+, which implements the value-inheritance property and avoids resetting the integral accumulator to zero upon mode-switching [19].*

Remark 2. *The integral value inheritance mechanism means that the accumulated integral information of the sliding surface will not be cleared when Markov mode-switching occurs [39]. By inheriting historical integral values, unexpected impulse fluctuations induced by mode jumps can be restrained, which is essential for SMJSs subject to spoofing attacks.*

3.3. SMC law design and reachability analysis

The following theorem synthesizes the state-estimation-based SMC scheme and can ensure that the state of dynamic systems can reach onto the constructed sliding surface $s(\hat{x}(t), g)$.

Theorem 1. *Consider the SMJS (1) with structured norm-bounded uncertainties $\Delta A_g = M_g F(t) N_g$, sliding mode observer (6), and mode-dependent integral sliding surface (8). We construct the following control scheme.*
(1) Neural SMC law

$$u(t) = \begin{cases} K_g\hat{x} - (B_g^{\mathrm{T}} G_g B_g)^{-1} B_g^{\mathrm{T}} G_g L_g(y - C_g\hat{x}) - \hat{R}^{\mathrm{T}}\Phi(\hat{H}^{\mathrm{T}}\bar{O}) - q_g(t)\dfrac{s}{\|s\|}, & s \neq 0; \\ K_g\hat{x} - (B_g^{\mathrm{T}} G_g B_g)^{-1} B_g^{\mathrm{T}} G_g L_g(y - C_g\hat{x}) - \hat{R}^{\mathrm{T}}\Phi(\hat{H}^{\mathrm{T}}\bar{O}), & s = 0. \end{cases} \tag{3.7}$$

(2) Observer-related robust compensation term

$$u_f(t) = \hat{R}^{\mathrm{T}}\Phi(\hat{H}^{\mathrm{T}}\bar{O}) + \hat{\alpha}^{\mathrm{T}}\Omega\,\mathrm{sgn}(s_c), \quad s_c = B_g^{\mathrm{T}} M_g e. \tag{3.8}$$

(3) NN weight adaptive laws

$$\dot{\hat{R}} = \Gamma_1(\Phi - \Phi'\hat{H}^{\mathrm{T}}\bar{O})s_c^{\mathrm{T}}, \quad \Gamma_1 > 0, \tag{3.9}$$

$$\dot{\hat{H}} = \Gamma_2\bar{O}s_c^{\mathrm{T}}\hat{R}^{\mathrm{T}}\Phi', \quad \Gamma_2 > 0. \tag{3.10}$$

(4) Residual bound adaptive law

$$\dot{\hat{\alpha}} = \Gamma_3\|s_c\|\Omega, \quad \Gamma_3 > 0. \tag{3.11}$$

(5) Switching gain

$$q_g(t) = \frac{1}{2\|s\|}\left\|\sum_{h=1}^{N}\lambda_{gh}s(\hat{x}, h)\right\| + \hat{\alpha}^{\mathrm{T}}\Omega + \varrho_g, \quad \varrho_g > 0. \tag{3.12}$$

Then the sliding variable $s(\hat{x}, g)$ converges to the sliding manifold $s(\hat{x}, g) = 0$ in finite-mean almost-sure time for any initial state and Markov mode.

Proof. Define the Lyapunov function for sliding dynamics:

$$V_1(\hat{x}, g) = \frac{1}{2}s^{\mathrm{T}}(\hat{x}, g)\left(B_g^{\mathrm{T}} G_g B_g\right)^{-1} s(\hat{x}, g). \tag{3.13}$$

Since B_g is the full-column rank and $G_g > 0$, and the matrix $B_g^{\mathrm{T}} G_g B_g$ is symmetric positive definite, so $V_1 \geq 0$ and $V_1 = 0$ if $s(\hat{x}, g) = 0$.

The weak infinitesimal generator of Markov process satisfies

$$\mathcal{L}V_1 = \frac{\partial V_1}{\partial \hat{x}}\dot{\hat{x}} + \sum_{h=1}^{N}\lambda_{gh}V_1(\hat{x}, h), \tag{3.14}$$

where λ_{gh} denotes the mode transition rate. Differentiate the sliding surface (8):

$$\dot{s} = B_g^{\mathrm{T}} G_g E\dot{\hat{x}} - B_g^{\mathrm{T}} G_g\left(A_g + M_g F(t) N_g + B_g K_g\right)\hat{x}. \tag{3.15}$$

Substitute the observer dynamics

$$E\dot{\hat{x}} = \left(A_g + M_g F(t) N_g\right)\hat{x} + B_g(u + u_f) + L_g(y - C_g\hat{x})$$

into (3.15), and simplify identical terms to obtain

$$\dot{s} = B_g^{\mathrm{T}} G_g\Big[B_g(u + u_f) + L_g(y - C_g\hat{x}) - B_g K_g\hat{x}\Big]. \tag{3.16}$$

Substitute the control law (3.7) and compensation term (3.8) into (3.16). The neural approximation term $\hat{R}^{\mathrm{T}}\Phi(\hat{H}^{\mathrm{T}}\bar{O})$ cancels completely, yielding

$$\dot{s} = -B_g^{\mathrm{T}} G_g B_g \frac{q_g(t)}{\|s\|} s + B_g^{\mathrm{T}} G_g B_g \hat{\alpha}^{\mathrm{T}}\Omega \mathrm{sgn}(s_c). \tag{3.17}$$

Left-multiply $s^{\mathrm{T}}\left(B_g^{\mathrm{T}} G_g B_g\right)^{-1}$ from (3.17) as follows:

$$s^{\mathrm{T}}\left(B_g^{\mathrm{T}} G_g B_g\right)^{-1}\dot{s} = -q_g(t)\|s\| + \hat{\alpha}^{\mathrm{T}}\Omega \cdot s^{\mathrm{T}}\mathrm{sgn}(s_c). \tag{3.18}$$

Substitute the switching gain (3.12) into (3.18). Note that $\hat{\alpha}^{\mathrm{T}}\Omega\left(s^{\mathrm{T}}\mathrm{sgn}(s_c) - \|s\|\right) \le 0$, and we get the upper bound

$$s^{\mathrm{T}}\left(B_g^{\mathrm{T}} G_g B_g\right)^{-1}\dot{s} \le -\frac{1}{2}\left\|\sum_{h=1}^{N}\lambda_{gh} s(\hat{x}, h)\right\| - \varrho_g\|s\|. \tag{3.19}$$

Combining (3.14) and (3.19), the Markovian jump's cross-term can satisfy

$$\sum_{h=1}^{N}\lambda_{gh} V_1(\hat{x}, h) \ge -\frac{1}{2}\left\|\sum_{h=1}^{N}\lambda_{gh} s(\hat{x}, h)\right\|,$$

thus the infinitesimal generator is bounded as

$$\mathcal{L}V_1 \le -\varrho_g\|s(\hat{x}, g)\|. \tag{3.20}$$

Let $\hbar_m = \max_{g\in\mathcal{A}}\lambda_{\max}\left(\left(B_g^{\mathrm{T}} G_g B_g\right)^{-1}\right) > 0$. From (3.13), we have

$$V_1 \le \frac{1}{2}\hbar_m\|s\|^2 \implies \|s\| \ge \sqrt{\frac{2V_1}{\hbar_m}}.$$

Substituting $V_1 \le \frac{1}{2}\hbar_m\|s\|^2 \implies \|s\| \ge \sqrt{\frac{2V_1}{\hbar_m}}$ into (3.20), it is seen that

$$\mathcal{L}V_1 \le -cV_1^{1/2}, \quad c = \varrho_g\sqrt{\frac{2}{\hbar_m}} > 0. \tag{3.21}$$

Inequality (3.21) meets the standard stochastic finite-time stability criterion with the exponent $1/2 \in (0)$. Separate variables and integrate from the initial time 0 to the hitting time τ_s ($V_1(\tau_s) = 0$):

$$\int_{V_1(0)}^{0} V_1^{-1/2} dV_1 \le -\int_0^{\tau_s} c\, dt \implies \tau_s \le \frac{2\sqrt{V_1(0)}}{c} < +\infty.$$

□

Remark 3. *It is worth pointing out the distinction between finite mean almost-sure time and deterministic finite-time stability. For deterministic finite-time stability, the settling time is bounded by a prescribed deterministic constant for all trajectories. However, the reaching instant here is a random stopping time [48]. The finite mean almost-sure time implies that reachability holds with probability of one, and the expectation of such a random stopping time is finite, whereas there is no uniform deterministic upper bound for individual sample paths.*

Remark 4. *The adaptive laws* (3.9)–(3.11) *act on the state estimation error* $e(t)$ *rather than the sliding variable* s. *The neural compensation item cancels out in sliding dynamics, so their time derivatives do not participate in the derivation of* $\mathcal{L}V_1$ *[13]. These adaptive updating rules will be utilized in the closed-loop stochastic admissibility proof of Theorem 2.*

3.4. Stochastic admissibility analysis

We start from the mode-dependent integral sliding surface given in (3.22):

$$s(\hat{x}(t), g) = B_g^T G_g E\hat{x}(t) - \int_0^t B_g^T G_g[A_g + M_g F(\tau)N_g + B_g K_g]\hat{x}(\tau)d\tau, \tag{3.22}$$

and the mode-dependent sliding-mode observer dynamics

$$E\dot{\hat{x}}(t) = [A_g + M_g F(t)N_g]\hat{x}(t) + B_g(u(t) + u_f(t)) + L_g(y(t) - C_g\hat{x}(t)), \tag{3.23}$$

where $\hat{x}(t)$ is the observed state, L_g denotes the observer gain matrix, and $u_f(t)$ is the robust compensation term for actuator attacks and NN approximation residuals.

Taking the time derivative of the sliding surface (3.22) yields

$$\dot{s}(\hat{x}, g) = B_g^T G_g E\dot{\hat{x}}(t) - B_g^T G_g[A_g + M_g F(t)N_g + B_g K_g]\hat{x}(t). \tag{3.24}$$

For ideal sliding mode motion on the sliding manifold, the sliding mode equivalent condition requires $\dot{s}(\hat{x}, g) = 0$. Substitute the observer dynamics (3.23) into (3.24) as follows:

$$\begin{aligned} \dot{s} =& B_g^T G_g\Big\{[A_g + M_g F(t)N_g]\hat{x} + B_g(u + u_f) + L_g(y - C_g\hat{x})\Big\} \\ &- B_g^T G_g[A_g + M_g F(t)N_g + B_g K_g]\hat{x}. \end{aligned} \tag{3.25}$$

The terms involving $(A_g + M_g F(t)N_g)\hat{x}(t)$ cancel out. Simplifying gives

$$\dot{s} = B_g^T G_g B_g(u(t) + u_f(t)) + B_g^T G_g L_g(y - C_g\hat{x}) - B_g^T G_g B_g K_g\hat{x}. \tag{3.26}$$

Set $\dot{s} = 0$ and let $u(t) = u_{\text{eq}}(t)$ for equivalent control on the sliding manifold:

$$0 = B_g^T G_g B_g(u_{\text{eq}}(t) + u_f(t)) + B_g^T G_g L_g(y - C_g\hat{x}) - B_g^T G_g B_g K_g\hat{x}.$$

Since B_g has full column rank and $G_g > 0$, the matrix $B_g^T G_g B_g$ is invertible. Rearranging and multiplying both sides by $(B_g^T G_g B_g)^{-1}$, we obtain the equivalent control law

$$u_{\text{eq}}(t) = K_g\hat{x} - (B_g^{\mathrm{T}} G_g B_g)^{-1} B_g^{\mathrm{T}} G_g L_g(y - C_g\hat{x}) - u_f(t). \tag{3.27}$$

Theorem 2. *Consider the sliding manifold $s(\hat{x}, g) = 0$ achieves finite-time reachability as established in Theorem 1. Substitute the equivalent control law*

$$u_{\mathrm{eq}}(t) = K_g\hat{x} - (B_g^{\mathrm{T}}G_gB_g)^{-1}B_g^{\mathrm{T}}G_gL_g(y - C_g\hat{x}) - u_f(t) \tag{3.28}$$

for the sliding mode observer (6), the resulting closed state and estimation error dynamics

$$\begin{aligned} E\dot{\hat{x}} &= (A_g + M_gF(t)N_g + B_gK_g)\hat{x} + (I - X_g)L_gC_ge, \\ X_g &\triangleq B_g(B_g^{\mathrm{T}}G_gB_g)^{-1}B_g^{\mathrm{T}}G_g, \end{aligned} \tag{3.29}$$

$$E\dot{e} = (A_g + M_gF(t)N_g - L_gC_g)e + B_g(\vartheta(x, t) - u_f(t)), \tag{3.30}$$

where the actuator attack signal $\vartheta(x, t) = R^{*T}\Phi(H^{*T}\bar{O})$ satisfies the bounded residual $\|\psi(x)\| \leq \alpha^{\mathrm{T}}\Omega$, and for all Markov modes, $g \in \mathcal{A}$. If there are positive definite matrices G_g, matrices P_g, M_g, and positive scalars ε_g, ν_g such that

$$P_g^{\mathrm{T}}E = E^{\mathrm{T}}P_g = E^{\mathrm{T}}G_gE \geq 0, \tag{3.31}$$

$$\begin{bmatrix} \Xi_{1g} & P_g^{\mathrm{T}}L_gC_g - P_g^{\mathrm{T}}X_gL_g \\ * & \Xi_{2g} \end{bmatrix} \leq 0, \tag{3.32}$$

with

$$\Xi\_1g = \mathrm{sym}(P_g^{\mathrm{T}}A_g) + \varepsilon_gP_gM_gM_g^{\mathrm{T}}P_g^{\mathrm{T}} + \varepsilon_g^{-1}N_g^{\mathrm{T}}N_g + \sum_{h=1}^{N}\lambda_{gh}E^{\mathrm{T}}G_hE + \nu_gI, \tag{3.33}$$

$$\Xi_{2g} = \mathrm{sym}(M_g^{\mathrm{T}}(A_g - L_gC_g)) + \varepsilon_gM_gM_g^{\mathrm{T}}M_g^{\mathrm{T}} + \varepsilon_g^{-1}N_g^{\mathrm{T}}N_g + \sum_{h=1}^{N}\lambda_{gh}M_h^{\mathrm{T}}E + \nu_gI, \tag{3.34}$$

then the closed-loop SMJS with structured uncertainties and actuator attacks is stochastically admissible. The NN adaptive laws

$$\dot{\hat{R}} = \Gamma_1(\Phi - \Phi'\hat{H}^{\mathrm{T}}\bar{O})s_c^{\mathrm{T}}, \quad \Gamma_1 > 0, \tag{3.35}$$

$$\dot{\hat{H}} = \Gamma_2\bar{O}s_c^{\mathrm{T}}\hat{R}^{\mathrm{T}}\Phi', \quad \Gamma_2 > 0, \tag{3.36}$$

$$\dot{\hat{\alpha}} = \Gamma_3\|s_c\|\Omega, \quad \Gamma_3 > 0, \quad s_c = B_g^{\mathrm{T}}M_ge, \tag{3.37}$$

are utilized to eliminate the approximation error of unknown attack nonlinearities in the stability analysis.

Proof. The proof consists of two separate parts: Regularity/impulse-free verification and mean-square stochastic stability analysis.

Part A: Regularity and impulse-free property. From Condition (3.31), perform standard singular decomposition for the rank-deficient matrix E. There are invertible matrices W_1, W_2 satisfying $W_1EW_2 = \mathrm{diag}\{I\_\sigma, 0\}$ with $\sigma = \mathrm{rank}(E)$. Partition the transformed matrices as

$$W_2^{\mathrm{T}}P_gW_1^{-1} = \begin{bmatrix} P_{11g} & P_{12g} \\ P_{21g} & P_{22g} \end{bmatrix}, \quad W_1(A_g + M_gFN_g)W_2 = \begin{bmatrix} A_{11g} & A_{12g} \\ A_{21g} & A_{22g} \end{bmatrix}.$$

The equality $E^{\mathrm{T}}P_g = P_g^{\mathrm{T}}E$ yields $P_{21g} = 0$. Applying the congruence transformation to (3.32) and extracting the bottom-right sub-block corresponding to zero rows/columns of E gives

$$P_{22g}A_{22g} + A_{22g}^{\mathrm{T}}P_{22g} < 0.$$

This negative-definite matrix implies A_{22g} is nonsingular for all admissible $F^{\mathrm{T}}F \leq I$. According to singular system theory, the matrix pair $(E, A_g + M_gFN_g)$ is regular and impulse-free for each mode g.

Part B: Mean-square stochastic stability. Construct the augmented Lyapunov functional incorporating state, error, and all neural adaptive estimation errors:

$$V_2(\hat{x}, e, \tilde{R}, \tilde{H}, \tilde{\alpha}, g) = \hat{x}^{\mathrm{T}}P_g^{\mathrm{T}}E\hat{x} + e^{\mathrm{T}}M_g^{\mathrm{T}}Ee + \mathrm{tr}(\tilde{R}^{\mathrm{T}}\Gamma_1^{-1}\tilde{R}) + \mathrm{tr}(\tilde{H}^{\mathrm{T}}\Gamma_2^{-1}\tilde{H}) + \tilde{\alpha}^{\mathrm{T}}\Gamma_3^{-1}\tilde{\alpha}, \tag{3.38}$$

where $\tilde{R} = \hat{R} - R^*$, $\tilde{H} = \hat{H} - H^*$, and $\tilde{\alpha} = \hat{\alpha} - \alpha$ denote the NN's weight and residual bound estimation errors. All quadratic terms are non-negative, and $V_2 = 0$ if and only if $\hat{x} = e = \tilde{R} = \tilde{H} = \tilde{\alpha} = 0$.

The weak infinitesimal generator of the Markov process acting on V_2 is split into five components:

$$\mathcal{L}V_2 = \mathcal{L}(\hat{x}^{\mathrm{T}}E^{\mathrm{T}}P_g\hat{x}) + \mathcal{L}(e^{\mathrm{T}}E^{\mathrm{T}}M_ge) + 2\mathrm{tr}(\tilde{R}^{\mathrm{T}}\Gamma_1^{-1}\dot{\hat{R}}) + 2\mathrm{tr}(\tilde{H}^{\mathrm{T}}\Gamma_2^{-1}\dot{\hat{H}}) + 2\tilde{\alpha}^{\mathrm{T}}\Gamma_3^{-1}\dot{\hat{\alpha}}. \tag{3.39}$$

(1) State term generator:

$$\mathcal{L}(\hat{x}^{\mathrm{T}}P_g^{\mathrm{T}}E\hat{x}) = \mathrm{sym}(\hat{x}^{\mathrm{T}}P_g^{\mathrm{T}}E\dot{\hat{x}}) + \sum_{h=1}^{N}\lambda_{gh}\hat{x}^{\mathrm{T}}P_h^{\mathrm{T}}E\hat{x}.$$

Substituting (3.29) and expand the structured uncertainty cross-term. Using the matrix inequality for bounded uncertainty, it is shown that

$$\mathrm{sym}(XMFN + N^{\mathrm{T}}F^{\mathrm{T}}M^{\mathrm{T}}X^{\mathrm{T}}) \leq \varepsilon XMM^{\mathrm{T}}X^{\mathrm{T}} + \varepsilon^{-1}N^{\mathrm{T}}N,$$

and the uncertainty contribution is absorbed into Ξ_1g defined in (3.33).

(2) Error term generator:

$$\mathcal{L}(e^{\mathrm{T}}M_g^{\mathrm{T}}Ee) = \mathrm{sym}(e^{\mathrm{T}}M_g^{\mathrm{T}}E\dot{e}) + \sum_{h=1}^{N}\lambda_{gh}e^{\mathrm{T}}M_h^{\mathrm{T}}Ee.$$

Substituting (3.30) and bounding the uncertainty bilinear term via the same scaling lemma yields the quadratic block Ξ_2g in (3.34). The cross-term $2e^{\mathrm{T}}M_g^{\mathrm{T}}B_g(\vartheta - u\_f)$ captures the uncompensated attack residual and will be fully canceled by adaptive derivatives.

(3) Neural adaptive law cancellation analysis. Recall the attack decomposition

$$\vartheta - \hat{R}^{\mathrm{T}}\Phi(\hat{H}^{\mathrm{T}}\bar{O}) = -\tilde{R}^{\mathrm{T}}(\Phi - \Phi'\hat{H}^{\mathrm{T}}\bar{O}) - \hat{R}^{\mathrm{T}}\Phi'\tilde{H}^{\mathrm{T}}\bar{O} - \psi(x),$$

and $u\_f = \hat{R}^{\mathrm{T}}\Phi(\hat{H}^{\mathrm{T}}\bar{O}) + \hat{\alpha}^{\mathrm{T}}\Omega\mathrm{sgn}(s_c)$. Substitute (3.35)–(3.37):

$$2\mathrm{tr}(\tilde{R}^{\mathrm{T}}\Gamma_1^{-1}\dot{\hat{R}}) = 2s_c^{\mathrm{T}}\tilde{R}^{\mathrm{T}}(\Phi - \Phi'\hat{H}^{\mathrm{T}}\bar{O}),$$

$$2\mathrm{tr}(\tilde{H}^{\mathrm{T}}\Gamma_2^{-1}\dot{\hat{H}}) = 2s_c^{\mathrm{T}}\hat{R}^{\mathrm{T}}\Phi'\tilde{H}^{\mathrm{T}}\bar{O},$$

$$2\tilde{\alpha}^{\mathrm{T}}\Gamma_3^{-1}\dot{\hat{\alpha}} = 2\|s\_c\|\tilde{\alpha}^{\mathrm{T}}\Omega, \quad -2s_c^{\mathrm{T}}\psi(x) \le -2\|s_c\|\alpha^{\mathrm{T}}\Omega.$$

Combining the attack cross-term and three adaptive items, we obtain

$$\begin{aligned}
&2e^{\mathrm{T}}M_g^{\mathrm{T}}B_g(\vartheta - u_f) + 2\mathrm{tr}(\tilde{R}^{\mathrm{T}}\Gamma_1^{-1}\dot{\hat{R}}) + 2\mathrm{tr}(\tilde{H}^{\mathrm{T}}\Gamma_2^{-1}\dot{\hat{H}}) + 2\tilde{\alpha}^{\mathrm{T}}\Gamma_3^{-1}\dot{\hat{\alpha}}\\
=& -2s_c^{\mathrm{T}}(\tilde{R}^{\mathrm{T}}(\Phi - \Phi'\hat{H}^{\mathrm{T}}\bar{O}) + \hat{R}^{\mathrm{T}}\Phi'\tilde{H}^{\mathrm{T}}\bar{O} + \psi(x)) + 2s_c^{\mathrm{T}}\tilde{R}^{\mathrm{T}}(\Phi - \Phi'\hat{H}^{\mathrm{T}}\bar{O})\\
&+ 2s_c^{\mathrm{T}}\hat{R}^{\mathrm{T}}\Phi'\tilde{H}^{\mathrm{T}}\bar{O} + 2\|s_c\|\tilde{\alpha}^{\mathrm{T}}\Omega\\
=& -2s_c^{\mathrm{T}}\psi(x) + 2\|s_c\|\tilde{\alpha}^{\mathrm{T}}\Omega \le 2\|s_c\|(\tilde{\alpha}^{\mathrm{T}} - \alpha^{\mathrm{T}})\Omega \le 0.
\end{aligned}$$

All neural weight cross-terms fully cancel, leaving a nonpositive residual bound.

After the LMI constraints (3.32), $\hbar_l > 0$ exists such that

$$\mathcal{L}V_2 \le -\hbar_l \left\| \begin{bmatrix} \hat{x}(t) \\ e(t) \end{bmatrix} \right\|^2 < 0. \tag{3.40}$$

Integrating over $[0, \infty)$ and taking the expectation for (3.40), it follows that

$$\mathbb{E}\left\{ \int_0^\infty \left\| \begin{bmatrix} \hat{x}(\tau) \\ e(\tau) \end{bmatrix} \right\|^2 d\tau \right\} \le \frac{1}{\hbar_l} V_2(\hat{x}(0), e(0), \tilde{R}(0), \tilde{H}(0), \tilde{\alpha}(0)) < \infty.$$

This satisfies the definition of mean-square stochastic stability. Combining Part A and Part B, the closed-loop system is stochastically admissible. □

Remark 5. *The matrix inequality conditions established in Theorem 2 have several nonlinear coupling terms, such as bilinear terms composed of the unknown matrix variables P_g and K_g, the reciprocal scalar coefficient ε_g^{-1}, and the matrix inversion term $(B_g^{\mathrm{T}}G_gB_g)^{-1}$. These nonlinear coupled inequalities are incompatible with mainstream LMI solvers, which only accept strict linear matrix inequality constraints without cross-matrix products and reciprocal parameters [22]. To convert the unsolvable coupled nonlinear constraints into tractable strict LMIs for numerical computation, we introduce auxiliary positive scalars l_g, ϵ_g and slack positive definite matrices S_g. By virtue of the Schur complement lemma and quadratic bounding inequalities, all nonlinear terms are decoupled equivalently. The subsequent Theorem 3 presents a set of fully linearized feasible LMI criteria to compute the observer gain L_g and the controller gain K_g [30].*

Theorem 3. *Consider the solving of Theorem 2. Define $X_g = B_g(B_g^{\mathrm{T}}G_gB_g)^{-1}B_g^{\mathrm{T}}G_g$. If the positive scalars ϵ_g, l_g, ν_g; the positive definite matrices G_g, S_g; and the matrices $\overline{K}_g, M_g, P_g$ exist such that the following two strict linear matrix inequalities are feasible:*

$$\begin{bmatrix}
\Lambda_{1g} & P_g^{\mathrm{T}} + \overline{K}_g^{\mathrm{T}}B_g^{\mathrm{T}} & P_g^{\mathrm{T}}A_g & P_g^{\mathrm{T}} & P_g^{\mathrm{T}}B_g & 0\\
* & -l_gI & 0 & 0 & 0 & 0\\
* & * & -\epsilon_gI & 0 & 0 & 0\\
* & * & * & -G_g & 0 & 0\\
* & * & * & * & -B_g^{\mathrm{T}}G_gB_g & 0\\
* & * & * & * & * & -\epsilon_gS_g
\end{bmatrix} < 0, \tag{3.41}$$

$$\begin{bmatrix}
\Lambda_{2g} & \sqrt{2}C_g^{\mathrm{T}}L_g^{\mathrm{T}}G_g\\
* & -G_g
\end{bmatrix} < 0, \tag{3.42}$$

where

$$\Lambda_{1g} = \mathrm{sym}(P_g^{\mathrm{T}} A_g) + \epsilon_g P_g M_g M_g^{\mathrm{T}} P_g^{\mathrm{T}} + \epsilon_g^{-1} N_g^{\mathrm{T}} N_g + \epsilon_g P_g^{\mathrm{T}} S_g^{-1} P_g \tag{3.43}$$

$$+ \sum_{h=1}^{N} \lambda_{gh} E^{\mathrm{T}} G_h E - 2P_g + \nu_g I, \tag{3.44}$$

$$\Lambda_{2g} = \mathrm{sym}(M_g^{\mathrm{T}}(A_g - L_g C_g)) + \epsilon_g M_g M_g^{\mathrm{T}} M_g^{\mathrm{T}} + \epsilon_g^{-1} N_g^{\mathrm{T}} N_g + \sum_{h=1}^{N} \lambda_{gh} M_h^{\mathrm{T}} E + \nu_g I, \tag{3.45}$$

then the matrix inequalities in Theorem 2 are solvable, and the state-feedback controller gain can be recovered as

$$K_g = \nu_g^{-1} \overline{K}_g. \tag{3.46}$$

The observer gain is fixed as $L_g = B_g B_g^{\mathrm{T}} C_g^{\mathrm{T}}$. The system with structured uncertainties $\Delta A_g = M_g F(t) N_g$ and actuator attacks satisfies stochastic admissibility.

Proof. The proof is divided into four core steps: Linearize bilinear controller cross-terms, eliminate reciprocal ϵ^{-1} via the Schur complement, decouple singular matrix coupling items, and reverse the Schur transformation to recover Theorem 2's LMI.

The original Ξ_{1g} in Theorem 2 contains the cross-term $\mathrm{sym}(P_g^{\mathrm{T}} B_g K_g)$, which couples the unknown matrices P_g, K_g and cannot be solved by standard LMI solvers. Introduce the substitution $\overline{K}_g = \nu_g K_g$, i.e., $K_g = \nu_g^{-1} \overline{K}_g$. Then

$$\mathrm{sym}(P_g^{\mathrm{T}} B_g K_g) = \nu_g^{-1} \mathrm{sym}(P_g^{\mathrm{T}} B_g \overline{K}_g).$$

Applying the standard matrix inequality for any scalar $l_g > 0$, shows that

$$\nu_g^{-1} \mathrm{sym}(P_g^{\mathrm{T}} B_g \overline{K}_g) \le l_g^{-1} P_g P_g^{\mathrm{T}} + l_g \nu_g^{-2} \overline{K}_g^{\mathrm{T}} B_g^{\mathrm{T}} B_g \overline{K}_g.$$

Move the positive semi-definite term to the left-hand side of the inequality, so the original negative definite condition remains valid if

$$\begin{aligned} &\mathrm{sym}(P_g^{\mathrm{T}} A_g) + \epsilon_g P_g M_g M_g^{\mathrm{T}} P_g^{\mathrm{T}} + \epsilon_g^{-1} N_g^{\mathrm{T}} N_g + \sum_{h=1}^{N} \lambda_{gh} E^{\mathrm{T}} G_h E - 2P_g + \nu_g I \\ &+ l_g^{-1} P_g P_g^{\mathrm{T}} + l_g \nu_g^{-2} \overline{K}_g^{\mathrm{T}} B_g^{\mathrm{T}} B_g \overline{K}_g < 0. \end{aligned}$$

This quadratic cross-term $l_g \nu_g^{-2} \overline{K}_g^{\mathrm{T}} B_g^{\mathrm{T}} B_g \overline{K}_g$ is transformed to off-diagonal blocks via the Schur complement to construct the second row and second column of (3.41).

The term $\epsilon_g^{-1} N_g^{\mathrm{T}} N_g$ in Λ_{1g} is nonlinear in ϵ_g. By the Schur complement lemma, we find that

$$\epsilon_g^{-1} N_g^{\mathrm{T}} N_g < \epsilon_g S_g \iff \begin{bmatrix} -\epsilon_g S_g & N_g^{\mathrm{T}} \\ * & -\epsilon_g I \end{bmatrix} < 0.$$

This block is embedded in the last row and last column of the large-scale LMI (3.41), removing the reciprocal ϵ_g^{-1} and converting to linear LMI constraints with the auxiliary matrix S_g. Similarly, the term $\epsilon_g P_g^{\mathrm{T}} S_g^{-1} P_g$ satisfies

$$\epsilon_g P_g^{\mathrm{T}} S_g^{-1} P_g < \epsilon_g^{-1} P_g P_g^{\mathrm{T}},$$

which is also embedded into the Schur block structure of (3.41).

The original LMI of Theorem 2 contains the nonlinear inverse term $(B_g^{\mathrm{T}} G_g B_g)^{-1}$. Applying the Schur complement, it follows that

$$\Psi - P_g^{\mathrm{T}} B_g (B_g^{\mathrm{T}} G_g B_g)^{-1} B_g^{\mathrm{T}} P_g < 0 \iff \begin{bmatrix} \Psi & P_g^{\mathrm{T}} B_g \\ * & -B_g^{\mathrm{T}} G_g B_g \end{bmatrix} < 0.$$

This block occupies the fifth row and fifth column of (3.41), fully eliminating the matrix inverse operation. The block with $-G$ (fourth diagonal entry) handles the singular matrix coupling term $E^{\mathrm{T}} G_h E$ from Markov jump summation.

Mixing cross-item $P_g^{\mathrm{T}} L_g C_g$ in Theorem 2's block LMI couples the observer gain L_g and the state matrix P_g. Split the coupled term via norm scaling, we get

$$\mathrm{sym}(P_g^{\mathrm{T}} L_g C_g) \leq 2 C_g^{\mathrm{T}} L_g^{\mathrm{T}} G_g L_g C_g,$$

which can be rewritten as the Schur complement form in (3.42):

$$\begin{bmatrix} \Lambda_{2g} & \sqrt{2} C_g^{\mathrm{T}} L_g^{\mathrm{T}} G_g \\ * & -G_g \end{bmatrix} < 0.$$

This small-scale LMI separates the observer gain L_g from state matrix P_g and the error matrix M_g.

If the LMIs (3.41) and (3.42) have feasible solutions, perform inverse Schur complement transformations in reverse order: (1) Eliminate the auxiliary matrices S_g, l_g to recover $\epsilon_g^{-1} N_g^{\mathrm{T}} N_g$ and bilinear controller bounds; (2) remove block terms containing the inverse of $B_g^{\mathrm{T}} G_g B_g$ to recover the original Ξ_{1g}, Ξ_{2g} blocks; and (3) recover the matrix equality constraint $P_g^{\mathrm{T}} E = E^{\mathrm{T}} P_g = E^{\mathrm{T}} G_g E \leq 0$ from the G_g block in (3.41).

If we substitute $K_g = \nu_g^{-1} \overline{K}_g$ back into the sliding surface and control law, then all matrix inequalities in Theorem 2 are satisfied. By combining this with the regularity and mean-square stability proof of Theorem 2, the closed-loop SMJS is stochastically admissible. □

4. Simulation

To verify the validity and superiority of the proposed mode-dependent adaptive neural SMC scheme, a DC motor's SMJS is taken as the numerical simulation object, which is widely adopted in mechanical drive modeling [19].

4.1. System modeling and parameter setting

The DC motor system is considered as the example, taken from [24]. As shown in Figure 2, the DC motor can drive a load, which may undergo random and sudden changes.

In this example, the DC motor's inductance L_m is neglected and the physical meaning and value of other parameters are shown in Table 1.

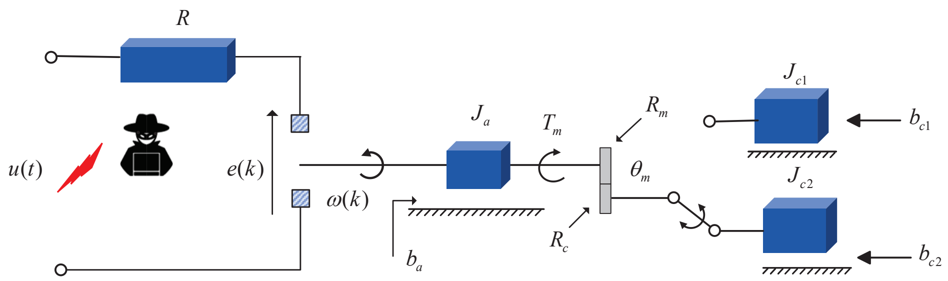

Figure 2. Block diagram of a DC motor.

Table 1. Parameters in the DC motor system

Parameter	Physical meaning	Value
R	Electric resistor	$1\,\Omega$
J_m	The moments of the motor	$0.5\,\mathrm{kg}\cdot\mathrm{m}$
J_{c1}	The moments of the Load 1	$50\,\mathrm{kg}\cdot\mathrm{m}$
J_{c2}	The moments of the Load 2	$150\,\mathrm{kg}\cdot\mathrm{m}$
b_a	The damping ratios	1
b_{c1}	The damping ratios	100
b_{c2}	The damping ratios	240

Denote $i(t)$ as the electric current, $w(t)$ as the speed of the shaft, and $u(t)$ as the voltage. According to the basic knowledge of circuits, we can see that

$$\begin{cases} \dot{w}(t) = -\dfrac{b_i}{J_i}w(t) + \dfrac{K_t}{J_i}i(t), \\ u(t) = K_w w(t) + Ri(t), \end{cases} \tag{4.1}$$

where K_w stands for the electromotive force constant and K_t represents the torque constant. J_i and b_i are calculated as

$$\begin{cases} J_i = J_m + \dfrac{J_{ci}}{n^2}, \\ b_i = b_m + \dfrac{b_{ci}}{n^2}. \end{cases} \tag{4.2}$$

Letting $x_1(t) = w(t)$ and $x_2(t) = i(t)$, and one has

$$\begin{bmatrix} 1 & 0 \\ 0 & 0 \end{bmatrix} \dot{x}(t) = \begin{bmatrix} -\dfrac{b_i}{J_i} & \dfrac{K_t}{J_i} \\ K_w & R \end{bmatrix} x(t) + \begin{bmatrix} 0 \\ -1 \end{bmatrix} u(t). \tag{4.3}$$

The system follows standard Markov jump process with two operation modes corresponding to light and heavy mechanical loads, and the transition rate matrix (constant, independent of the dwell time) is given by

$$\Lambda = \begin{bmatrix} -1.7725 & 1.7725 \\ 2.7082 & -2.7082 \end{bmatrix}.$$

For $r_t = i \in \{1, 2\}$, we simplify $A(r_t) = A_i$, $\Delta A(r_t, t) = \Delta A_i(t)$, $B(r_t) = B_i$, $C(r_t) = C_i$. The structured uncertainty satisfies $\Delta A_i(t) = M_i F(t) N_i$, $F^{\mathrm{T}}(t)F(t) \leq I$. Mode-dependent nominal matrices:

$$A_1 = \begin{bmatrix} -2 & 6 \\ 1 & 10 \end{bmatrix}, \quad A_2 = \begin{bmatrix} -0.016 & 0.02 \\ 1 & 10 \end{bmatrix}, \quad B_1 = B_2 = \begin{bmatrix} 0 \\ -1 \end{bmatrix}, \quad C_1 = C_2 = \begin{bmatrix} 1 & 0 \end{bmatrix}.$$

Uncertainty matrices:

$$M\_1 = \begin{bmatrix} 0.1 & 0 \\ 0 & 0.1 \end{bmatrix}, \ N_1 = \begin{bmatrix} 0.1 & 0 \\ 0.2 & 0.1 \end{bmatrix}, \ F_1(t) = 0.3 \cos t,$$

$$M_2 = \begin{bmatrix} 0.1 & 0.2 \\ 0 & 0.1 \end{bmatrix}, \ N_2 = \begin{bmatrix} 0.1 & 0 \\ 0.2 & 0 \end{bmatrix}, \ F_2(t) = 0.4 \sin t.$$

Unknown nonlinear actuator attack without pre-known bounded constraint:

$$\psi(x(t), t) = 0.5 \sqrt{x_1^2(t) + x_2^2(t)} \cos t.$$

A three-layer feedforward NN with 20 hidden neurons is adopted to approximate $\psi(x, t)$, activation function $\sigma_s(x_s) = \dfrac{1}{1 + e^{-a_s x_s}}$, and $a_s > 0$. The neural approximation error satisfies $\|\varepsilon(x)\| \leq \mu$.

4.2. Control and adaptive parameter configuration

(1) The NN's initial parameters and adaptive gains are as follows: Initial weights $\hat{W}(0) = \mathbf{0}_{20\times1}$, $\hat{V}(0) = \mathbf{0}_{3\times20}$; the residual bound $\hat{\alpha}(0) = \mathbf{0}_{4\times1}$; the adaptive matrices $\Gamma_1 > 0, \Gamma_2 > 0, \Gamma_3 > 0$ are identity matrices of matching dimensions. (2) The LMI solution parameters are: Positive scalars $\epsilon_i > 0, \nu_i > 0, \zeta_i > 0$. After solving the minimization optimization subject to strict LMIs in Theorem 3, the equality constraint $B_i^{\mathrm{T}} Q_i = H_i C_i$ is approximately satisfied with the minimum residuals $\epsilon_1 = 4.7210 \times 10^{-16}$, $\epsilon_2 = 5.0380 \times 10^{-13}$. (3) Solved Lyapunov and controller matrices

$$X_1 = \begin{bmatrix} 1.4993 & -0.2263 \\ -0.2263 & 6.1090 \end{bmatrix}, \quad X_2 = \begin{bmatrix} 2.0625 & -0.0638 \\ -0.0638 & 5.3295 \end{bmatrix},$$

the state feedback gains $K_1 = \begin{bmatrix} -0.5610 & -1.6654 \end{bmatrix}$ and $K_2 = \begin{bmatrix} 0.0700 & -1.4593 \end{bmatrix}$; and the observer gain $L_i = B_i B_i^{\mathrm{T}} C_i^{\mathrm{T}}$. (4) Chattering suppression: Replace the discontinuous sign function with the saturation approximation $\mathrm{sat}(\cdot) = \dfrac{\cdot}{\| \cdot \| + 0.01}$ to eliminate high-frequency chatter in practical control signals. (5) Simulation setup: Initial true state $x(0) = \begin{bmatrix} -0.5 & 0.5 \end{bmatrix}^{\mathrm{T}}$, and an initial estimation $\hat{x}(0) = \begin{bmatrix} -0.45 & 0.45 \end{bmatrix}^{\mathrm{T}}$. Total simulation time is 5 s, with a fixed integration step of 0.001 s.

4.3. Simulation result analysis

4.3.1. State and estimation curves

Figure 3 plots the actual state $x(t)$ and observer reconstruction $\hat{x}(t)$. Subject to time-varying structured uncertainties and nonlinear actuator attacks, the proposed mode-dependent sliding observer realizes fast state tracking within 0.3 s. Local magnified subfigures verify the rapid convergence of both speed and current signals.

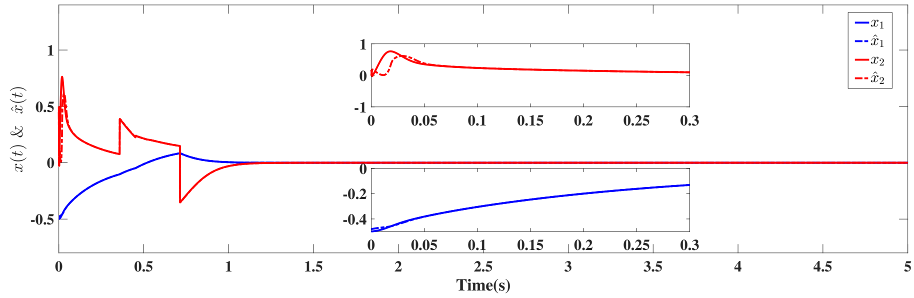

Figure 3. State response $x(t)$ and state estimation response $\hat{x}(t)$.

4.3.2. State estimation error

Figure 4 illustrates the estimation error $e(t) = x(t) - \hat{x}(t)$. The error converges to a tiny neighborhood of zero instantly and maintains small fluctuations during all Markov switching instants, demonstrating the strong disturbance rejection of the designed observer.

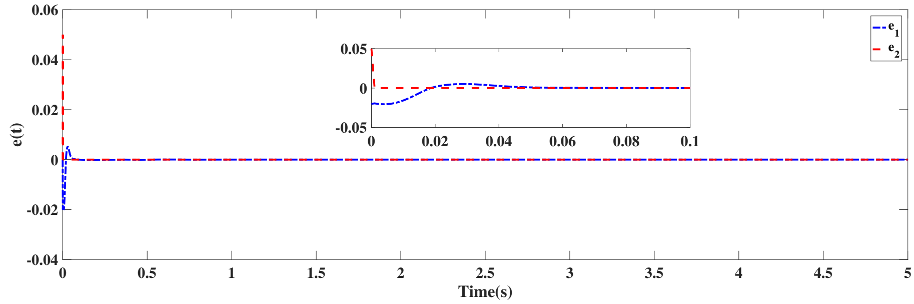

Figure 4. Error response $e(t)$.

4.3.3. Sliding variable trajectory

Figure 5 presents the evolution of the sliding signal $s(t)$. The sliding manifold $s = 0$ is reached in finite time and maintained for the whole simulation interval, which validates the finite-time reachability conclusion derived in Theorem 1.

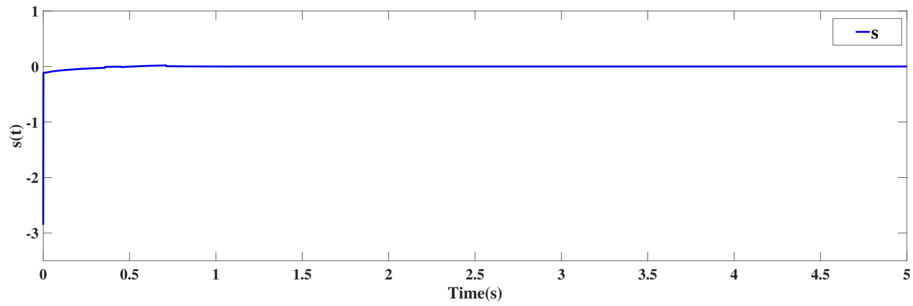

Figure 5. Sliding variable $s(t)$.

4.3.4. Control input signal

Figure 6 displays the designed control voltage $u(t)$. Benefiting from saturation approximation, the control input only has mild transient oscillation at the initial stage and a smooth steady response without severe chattering, satisfying the hardware implementation requirements of DC motor drive circuits.

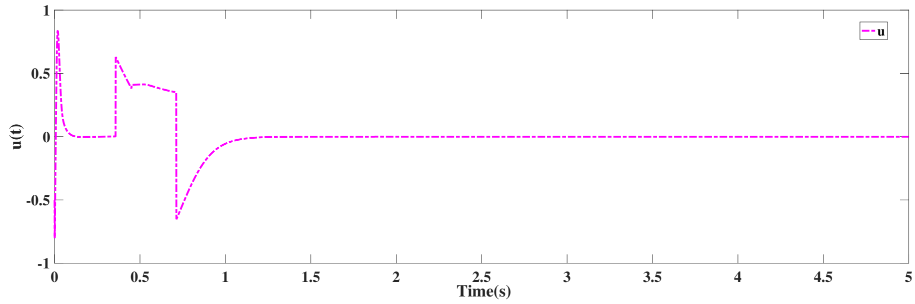

Figure 6. Control input $u(t)$.

4.3.5. Evolution of adaptive neural weights

Figures 7–9 depict the norm of the adaptive parameters $||\hat{R}(t)||$, $||\hat{H}(t)||$, and $||\hat{\alpha}(t)||$, respectively. All adaptive variables converge to steady constant values after a short transient process, which proves that the proposed adaptive laws can online adjust neural weights to compensate for unknown attacks' nonlinearity.

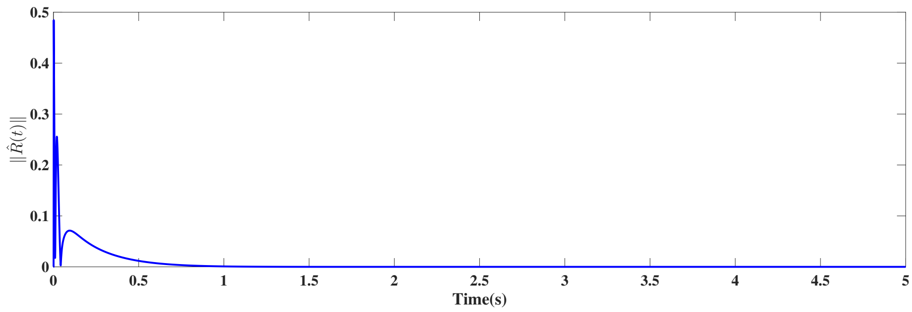

Figure 7. Adaptive parameter $||\hat{W}(t)||$.

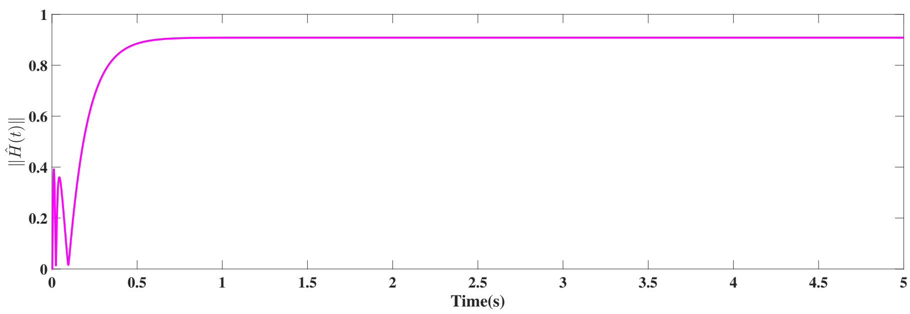

Figure 8. Adaptive parameter $||\hat{V}(t)||$.

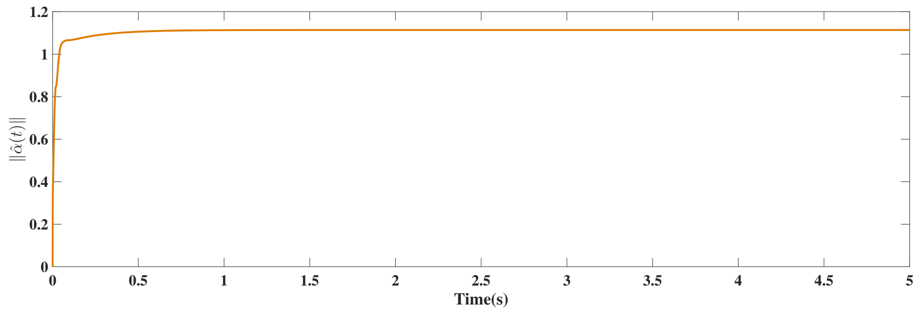

Figure 9. Adaptive parameter $||\hat{\alpha}(t)||$.

As shown in Figures 7–9, slight transient fluctuations can be observed in the norms of the adaptive neural weights $||\hat{R}(t)||$, $||\hat{H}(t)||$, and the adaptive residual-bound parameter $||\hat{\alpha}(t)||$ at the initial stage and Markovian mode-switching moments. These fluctuations mainly stem from two factors. First, the system undergoes time-varying structured parametric uncertainties and unknown nonlinear actuator spoofing attacks, which continuously excite the adaptive update laws. Second, Markovian mode transitions change the system's dynamics, bringing abrupt variations to the driving signal s_c of the adaptive rules. After the transient phase, all adaptive parameters gradually converge to steady values, which indicates that the NN can complete online parameter tuning for attack compensation.

4.3.6. Approximation performance of an actuator attack

Figure 10 compares a real attack $\psi(x,t)$ and a neural estimation $\hat{\psi}(x,t)$. Without prior upper-bound information of the attack signals, the feedforward NN achieves accurate online approximation and eliminates the adverse impact of malicious injection on the system's stability.

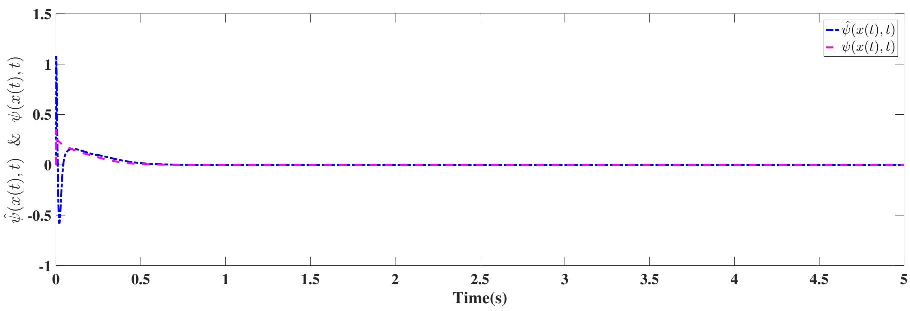

Figure 10. Actuator attack $\psi(x(t),t)$ and its estimate $\hat{\psi}(x(t),t)$

5. Conclusions

In this paper, we have studied the finite mean almost-sure reachability for SMJSs under spoofing attacks. A dynamic-memory event-triggered protocol has been adopted to reduce network load and defend against malicious signal tampering. A mode-dependent integral sliding surface with integral inheritance has been constructed to suppress the impulse fluctuations induced by Markov mode-switching, and a NN approximator has been utilized to compensate for unknown non-linearities. Sufficient reachability conditions have been established via coupled matrix inequalities in the sense of finite mean almost-sure time. A DC motor simulation has validated the effectiveness of the proposed control scheme. Nevertheless, this approach has had some limitations. The NN approximator introduced extra computational overhead. For high-dimensional systems, rising computational complexity hinders real-time onboard implementation. Moreover, the theoretical results have relied on the solvability of the derived coupled matrix inequalities. Future work will aim to reduce the computational cost for high-dimensional cases. This framework will also be extended to systems with partially known transition rates and hybrid multiple cyber-attacks.

Author contributions

Zhihao Wang: Conceptualization, Formal analysis, Writing–original draft; Xuetong Zhang: Software, methodology, Writing–review and editing; Zihan Zhao: Formal analysis, Writing-review and editing; Guangming Zhuang: Validation, Vvisualization. All authors have approved the final manuscript for publication.

Use of AI tools declaration

The authors declare they have not used Artificial Intelligence (AI) tools in the creation of this article.

Acknowledgments

The authors would like to thank the editors and the anonymous reviewers for their strict analysis and valuable comments and suggestions, which greatly improved the quality, scientific value and readability of the paper. This work was partly supported by the National Natural Science Foundation of China under Grants 62173174 and 61773191; the Shandong Provincial Natural Science Foundation under Grants ZR2024MF081, and ZR2023QF098 ; the Postgraduate Education Quality Improvement Plan Project of Liaocheng University under Grant LCUJYZD2501; the Graduate Education High-Quality Curriculum Construction Project for Shandong Province-Introduction to Systems Science under Grant SDYKC2024168.

Conflict of interest

The authors declare that they have no conflict of interest.

References

1. S. Xu, J. Lam, *Robust Control and Filtering of Singular Systems*, Berlin: Springer, 2006.
2. Z. Feng, H. Zhang, W. X. Zheng, PD control-based reachable set synthesis for singular Takagi–Sugeno fuzzy systems with time-varying delay, *IEEE Trans. Cybern.*, **54** (2024), 254–264. https://doi.org/10.1109/TCYB.2022.3210184
3. M. Maghenem, E. Panteley, A. Loría, Singular-perturbations-based analysis of dynamic consensus in directed networks of heterogeneous nonlinear systems, *IEEE Trans. Autom. Control*, **69** (2024), 4475–4490. https://doi.org/10.1109/TAC.2023.3327931

4. T. Saravanakumar, A. Stephen, X. Bai, Q. Zhu, T. Huang, New results on memory sampled-data control design for IT2 fuzzy singular systems with external disturbance, *IEEE Trans. Cybern.*, **56** (2026), 788–801. https://doi.org/10.1109/TCYB.2025.3607281

5. C. Zhang, B. Kao, C. Wang, B. Liu, Y. Kao, Observer-based event-triggered sliding mode control for delayed semi-Markov jump discrete singular systems under false data injection attacks, *IEEE Trans. Autom. Sci. Eng.*, **23** (2026), 1021–1031. https://doi.org/10.1109/TASE.2025.3643820

6. G. Zhuang, J. Xia, J. Feng, Y. Wang, G. Chen, Dynamic compensator design and H∞ admissibilization for delayed singular jump systems via Moore–Penrose generalized inversion technique, **49** (2023), 101361. https://doi.org/10.1016/j.nahs.2023.101361

7. L. Qiu, J. Zhao, Adaptive designated-time fuzzy event-triggered tracking of constrained nonlinear systems and its applications in robotic systems, *AIMS Math.*, **11** (2026), 15691–15715. https://dx.doi.org/10.3934/math.2026645

8. M. Xing, Y. Wang, G. Zhuang, F. Chen, Event-based asynchronous and resilient filtering for singular Markov jump LPV systems against deception attacks, *Appl. Math. Comput.*, **403** (2021), 126176. https://doi.org/10.1016/j.amc.2021.126176

9. X. Wang, G. Zhuang, G. Chen, Q. Ma, J. Lu, Asynchronous mixed H∞ and passive control for fuzzy singular delayed Markovian jump system via hidden Markovian model mechanism, *Appl. Math. Comput.*, **429** (2022), 127253. https://doi.org/10.1016/j.amc.2022.127253

10. A. Miranville, R. Quintanilla, Parabolic phase-lag heat conduction theories revisited, *Appl. Math. Lett.*, **133** (2022), 108264. https://doi.org/10.1016/j.aml.2022.108264

11. W. Zhang, G. Pang, X. Chen, X. Mou, J. Qiu, J. Cao, Projective group consensus fault-tolerant control for multi-agent systems under time-varying polynomial faults and input constraints, *Commun. Nonlinear Sci. Numer. Simul.*, **161** (2026), 110208. https://doi.org/10.1016/j.cnsns.2026.110208

12. X. Wu, W. Sun, Adaptive fault tolerant optimal control for high-order fully actuated system and its application in spacecraft attitude tracking using reinforcement learning, *Appl. Math. Comput.*, **512** (2026), 129774. https://doi.org/10.1016/j.amc.2025.129774

13. L. Zhang, H. Wang, Y. Zhu, J. Yang, Tube-based attitude control of rigid-bodies with magnitude-bounded disturbances, *Automatica*, **133** (2021), 109845. https://doi.org/10.1016/j.automatica.2021.109845

14. T. Wu, J. Cao, L. Xiong, J. H. Park, H. K. Lam, Reinforcement learning for fuzzy structured adaptive optimal control of discrete-time nonlinear complex networks, *IEEE Trans. Fuzzy Syst.*, **32** (2024), 6035–6043. https://doi.org/10.1109/TFUZZ.2024.3434690

15. Y. Gao, W. Sun, S. F. Su, Prescribed-time adaptive output feedback tracking control for nonlinear systems with quantized input, *Appl. Math. Comput.*, **463** (2024), 128370. https://doi.org/10.1016/j.amc.2023.128370

16. J. Xia, J. Zhang, W. Sun, B. Zhang, Z. Wang, Finite-time adaptive fuzzy control for nonlinear systems with full state constraints, *IEEE Trans. Syst. Man Cybern.: Syst.*, **49** (2018), 1541–1548. https://doi.org/10.1109/TSMC.2018.2854770

17. G. Chen, J. Xia, J. H. Park, H. Shen, G. Zhuang, Sampled-data synchronization of stochastic Markovian jump neural networks with time-varying delay, *IEEE Trans. Neural Netw. Learn. Syst.*, **33** (2022), 3829–3841. https://doi.org/10.1109/TNNLS.2021.3054615

18. Y. Wu, G. Zhuang, M. Jiang, Y. Wang, H∞ adaptive ETF control for degenerate jump systems under actuator faults and impulsive deception attacks with application to DCMIP device, *Appl. Math. Comput.*, **489** (2025), 129158. https://doi.org/10.1016/j.amc.2024.129158

19. Y. Qin, X. Han, A. Miranville, Existence of time-dependent global attractors for a wave equation with nonlinear boundary dissipation and boundary sources with critical exponents, *J. Differ. Equ.*, **470** (2026), 114345. https://doi.org/10.1016/j.jde.2026.114345

20. Y. Liu, G. Zhuang, J. Zhao, J. Lu, Z. Wang, H∞ admissibilization for time-varying delayed nonlinear singular impulsive jump systems based on memory state-feedback control, *Appl. Math. Comput.*, **447** (2023), 127921. https://doi.org/10.1016/j.amc.2023.127921

21. Q. Wang, B. Fu, C. Lin, P. Li, Exponential synchronization of chaotic Lur'e systems with time-triggered intermittent control, *Commun. Nonlinear Sci. Numer. Simul.*, **109** (2022), 106298. https://doi.org/10.1016/j.cnsns.2022.106298

22. Y. Zhao, G. Pang, X. Chen, J. Qiu, J. Cao, Robust fault-tolerant control for switched systems based on adaptive unknown input observer, *Commun. Nonlinear Sci. Numer. Simul.*, **140** (2025), 108416. https://doi.org/10.1016/j.cnsns.2024.108416

23. M. Hao, G. Zhuang, G. Cui, J. Xia, Observer-based dynamic event-triggered finite-time switching control for networked discrete implicit DC circuit systems under aperiodic DoS attacks, *IEEE Trans. Autom. Sci. Eng.*, **22** (2025), 22925–22937. https://doi.org/10.1109/TASE.2025.3624969

24. H. Wang , J. Yang, Y. Liang, Y. Zhu, L. Zhang, Guaranteed cost control of rigid-body attitude systems under control saturation, *Int. J. Robust Nonlinear Control*, **31** (2020), 2393–2410. https://doi.org/10.1002/rnc.5397

25. L. Zhu, Y. Wang, G. Zhuang, G. Song, Dynamic-memory event-based asynchronous dissipative filtering for T-S fuzzy singular semi-Markov jump systems against multi-cyber attacks, *Appl. Math. Comput.*, **431** (2022), 127352. https://doi.org/10.1016/j.amc.2022.127352

26. Y. Kao, Y. Li, J. H. Park, X. Chen, Mittag–Leffler synchronization of delayed fractional memristor neural networks via adaptive control, *IEEE Trans. Neural Netw. Learn. Syst.*, **32** (2021), 2279–2284. https://doi.org/10.1109/TNNLS.2020.2995718

27. H. Zhang, G. Zhuang, W. Sun, Y. Li, J. Lu, pth moment asymptotic interval stability and stabilization of linear stochastic systems via generalized H-representation, *Appl. Math. Comput.*, **386** (2020), 125520. https://doi.org/10.1016/j.amc.2020.125520

28. Z. Zhao, R. Hu, J. Zhang, G. Wang, G. Ma, H. Xia, Predefined-time optimal control for 6-DOF air-bearing testbed formation system: learning enhancement and disturbance compensation, *Nonlinear Dyn.*, **113** (2024), 19475–19504. https://doi.org/10.1007/s11071-025-11194-0

29. Y. Zhang, X. Li, T. Zhang, H. Zhang, Variable convergence rate fuzzy control of chaotic Chua's circuit under impulsive and stochastic disturbances, *AIMS Math.*, **11** (2026), 3703–3723. https://doi.org/10.3934/math.2026150

30. Y. Liu, G. Zhuang, X. Xie, Q. Ma, Impulsive observer-based admissibilization for delayed degenerate jump systems and application to DCM-IP device, *Nonlinear Anal.: Hybrid Syst.*, **50** (2023), 101395. https://doi.org/10.1016/j.nahs.2023.101395
31. J. Zhao, Y. Yuan, Z. Y. Sun, X. Xie, Applications to the dynamics of the suspension system of fast finite time stability in probability of p-norm stochastic nonlinear systems, *Appl. Math. Comput.*, **457** (2023), 128221. https://doi.org/10.1016/j.amc.2023.128221
32. T. Wu, J. Cao, J. H. Park, K. Shi, L. Xiong, T. Huang, Attack-resilient dynamic event-triggered synchronization of fuzzy reaction–diffusion dynamic networks with multiple cyberattacks, *IEEE Trans. Fuzzy Syst.*, **32** (2024), 498–509. https://doi.org/10.1109/TFUZZ.2023.3300882
33. H. Zhang, Y. Dai, C. Zhu, Region stability analysis and precise tracking control of linear stochastic systems, *Appl. Math. Comput.*, **465** (2024), 128402. https://doi.org/10.1016/j.amc.2023.128402
34. T. Yang, Z. Wang, X. Huang, J. Xia, G. Chen, Aperiodic sampled-data controller design for stochastic Markovian jump systems and its application, *Int. J. Robust Nonlinear Control*, **31** (2021), 6721–6739. https://doi.org/10.1002/rnc.5654
35. Y. Liu, G. Zhuang, W. Sun, J. Zhao, Y. Chu, Resilient H∞ dynamic output feedback controller design for USJSs with time-varying delays, *Appl. Math. Comput.*, **395** (2021), 125875. https://doi.org/10.1016/j.amc.2020.125875
36. J. Zhao, H. Zhao, Y. Song, Z. Y. Sun, D. Xiu, Fast finite-time consensus protocol for high-order nonlinear multi-agent systems based on event-triggered communication scheme, *Appl. Math. Comput.*, **508** (2026), 129631. https://doi.org/10.1016/j.amc.2025.129631
37. Y. Cao, J. Zhao, Z. Sun, State feedback stabilization problem of stochastic high-order and low-order nonlinear systems with time-delay, *AIMS Math.*, **8** (2023), 3185–3203. https://doi.org/10.3934/math.2023163
38. G. Chen, G. Du, K. Liu, J. Xia, J. H. Park, Asynchronous networked control with multisensor fusion: A hybrid framework for active suspension optimization, *IEEE Trans. Control Syst. Technol.*, **34** (2026), 2061–2072. https://doi.org/10.1109/TCST.2026.3685684
39. Y. Pang, G. Zhuang, J. Xia, X. P. Xie, H_∞ security control for singular jump systems with actuator faults and DoS attacks under switching-like adaptive trigger and application to OCCP, *IEEE Trans. Autom. Sci. Eng.*, **22** (2025), 7955–7966. https://doi.org/10.1109/TASE.2024.3475374
40. Y. Wang, J. Xia, H. Shen, J. Cao, HMM-based quantized dissipative control for 2-D Markov jump systems, *Nonlinear Anal.: Hybrid Syst.*, **40** (2021), 101018. https://doi.org/10.1016/j.nahs.2021.101018
41. X. Meng, Z. Li, J. Cao, Image encryption via sliding mode synchronization of fractional-order quaternion-valued T-S fuzzy neural networks with uncertain parameters, *IEEE Trans. Fuzzy Syst.*, **34** (2026), 489–502. https://doi.org/10.1109/TFUZZ.2025.3639056
42. Y. Kao, X. Feng, J. Xie, B. Kao, Event-triggered fault-tolerant sliding mode control for discrete Markov jump systems via guaranteed cost control approach, *IEEE Trans. Cir. Syst. II: Express Briefs*, **71** (2024), 3363–3367. https://doi.org/10.1109/TCSII.2023.3342065

43. D. Ren, G. Pang, X. Mou, X. Chen, J. Qiu, J. Cao, Simultaneous fault-tolerant consensus control and disturbance suppression for multi-agent systems with polynomial form fault under switching topology, *Syst. Control Lett.*, **193** (2024), 105946. https://doi.org/10.1016/j.sysconle.2024.105946

44. G. Zhuang, Z. Wang, X. Xie, J. Xia, Embedded-adaptive-observer-based H_∞ integrated fault estimation and memory fault-tolerant control for nonlinear delayed implicit robotic arm, *IEEE Trans. Indust. Inform.*, **20** (2024), 8317–8327. https://doi.org/10.1109/TII.2024.3372009

45. J. Xia, H. Yue, J. Zhang, J. H. Park, Fully distributed optimization algorithm for nonlinear multiagent systems under stochastic event-triggered mechanism, *IEEE Trans. Indust. Inform.*, **21** (2025), 8248–8257. https://doi.org/10.1109/TII.2025.3586059

46. Y. Liu, G. Pang, J. Qiu, X. Chen, J. Cao, Fault-tolerant control for output regulation in multi-agent systems based on prescribed-time observers, *IEEE Trans. Signal Inform. Proc. Netw.*, **10** (2024), 729–739. https://doi.org/10.1109/TSIPN.2024.3458789

47. T. Yang, G. Chen, J. Xia, Z. Wang, Q. Sun, Robust H_∞ filtering for polytopic uncertain stochastic systems under quantized sampled outputs, *Appl. Math. Comput.*, **347** (2019), 688–701. https://doi.org/10.1016/j.amc.2018.11.035

48. X. Meng, Z. Li, J. Cao, Almost periodic quasi-projective synchronization of delayed fractional-order quaternion-valued neural networks, *Neural Netw.*, **169** (2024), 92–107. https://doi.org/10.1016/j.neunet.2023.10.017

49. K. Fan, G. Pang, X. Chen, J. Qiu, J. Cao, Fault-tolerant control of multi-agent systems using a Fourier series observer under DoS attacks and periodic intermittent faults, *Syst. Control Lett.*, **211** (2026), 106397. https://doi.org/10.1016/j.sysconle.2026.106397

50. G. Zhuang, Y. Liu, J. Xia, X. P. Xie, Normalized P-D and intermittent hybrid H_∞ control for delayed descriptor systems via impulsive-inputs-dependent conditions, *IEEE Trans. Autom. Sci. Eng.*, **22** (2025), 3125–3134. https://doi.org/10.1109/TASE.2024.3389983

51. T. Wu, J. Cao, C. K. Ahn, L. Xiong, Y. Liu, H. K. Lam, Anti-attack protocol-based synchronization control for fuzzy complex dynamic networks, *IEEE Trans. Fuzzy Syst.*, **32** (2024), 3433–3443. https://doi.org/10.1109/TFUZZ.2024.3373440

52. G. Chen, X. Liu, X. Ren, J. Xia, J. H. Park, Asynchronous-based countermeasure for stealthy attack on aperiodic sampled-data control systems, *IEEE Trans. Autom. Control*, **70** (2025), 6159–6166. https://doi.org/10.1109/TAC.2025.3552745